



## ÇALDIRAN FAY ZONU VE CIVARINDAKİ COULOMB STRESS TRANSFERİ VE DEPREM TEHLİKESİ ANALİZİ

Hamdi ALKAN<sup>1\*</sup>, Serkan ÖZTÜRK<sup>2</sup>, İsmail AKKAYA<sup>1</sup>

<sup>1</sup> Van Yüzüncü Yıl Üniversitesi, Mühendislik Fakültesi, Jeofizik Mühendisliği Bölümü, Van, Türkiye

<sup>2</sup> Gümüşhane Üniversitesi, Mühendislik ve Doğa Bilimleri Fakültesi, Jeofizik Mühendisliği Bölümü, Gümüşhane, Türkiye

Anahtar Kelimeler	Öz
<i>Çaldıran Fay Zonu, B-Değeri, Deprem Olasılığı, Tekrarlama Zamanı, Coulomb Gerilme Değişimi.</i>	<p>Çaldıran fay zonu (CFZ) bir çok yıkıcı deprem üreten ve deprensellik açısından önemli bir aktif zondur. Bu fay sisteminde, 1976 tarihinde bu yıkıcı depremlerin en sonuncusu (<math>M_s = 7.3</math>) meydana gelmiştir. Dolayısıyla bu fay zonunda sismotektonik <math>b</math>-değeri, deprem olasılığı, tekraralama zamanı ve Coulomb gerilme değişimi parametrelerine bağlı olarak gelecek deprem potansiyeli ve pozitif/negatif gerilme değişimleri araştırılmıştır. Büyüklüğü 3.6'dan büyük olan depremler, sismotektonik parametrelerle ilgili olarak gerilme transfer yönünü araştırmak için kullanılmıştır. Çalışmanın sonuçlarına göre, CFZ'nin güneydoğusu boyunca küçük <math>b</math> değerleri elde edilmişken, büyük <math>b</math> değerleri Van Gölünün doğusu civarında hesaplanmıştır. Diğer taraftan, CFZ'nin kuzeydoğusu mevcut stress birikimini temsil etmektedir. Benzer şekilde, 1976 depreminin Coulomb gerilme değişimi bu fay sisteminin kuzeybatısında gerilmelerin farklı derinliklerde biriktiğini göstermektedir. Ayrıca, daha önceki çalışmalarda uzun dönem kayma oranları ve yatay öteleme değerleri dikkate alındığında, 6.0'dan büyük bir deprem için tekraralama zamanı yaklaşık 302 yıldır. Sonuç olarak, bu karşılaştırmalı analizler bölgede sismik tehlike değerlendirmesinin etkilerini ve olası bir sonraki deprem oluşumunun tahminini açıklamaktadır.</p>

## ANALYSIS OF COULOMB STRESS TRANSFER AND EARTHQUAKE HAZARD IN THE ÇALDIRAN FAULT ZONE AND ITS ADJACENT REGION

Keywords	Abstract
<i>Çaldıran Fault Zone, B-Value, Earthquake Probability, Recurrence Time, Coulomb Stress Variation.</i>	<p>Çaldıran fault zone (CFZ) are significant seismically active zone that generated many destructive earthquakes. In this fault system, the last of these major earthquakes occurred on 1976 (<math>M_s = 7.3</math>). Therefore, based on the seismotectonic <math>b</math>-value, earthquake probability, recurrence times and Coulomb stress changes, we investigate the future earthquake potential and positive/negative stress changes in this fault zone. The events with a magnitude greater than 3.6 are used to investigate stress transfer direction regarding the seismotectonic parameters. The results indicate that the regions having smaller <math>b</math>-values are obtained along with the SE of CFZ, whilst higher <math>b</math>-values are calculated around the east of Lake Van. On the other hand, the northeast of CFZ represents current stress accumulation. Similarly, the Coulomb stress variations of 1976 earthquake show that stress accumulated at different depths in the northwest of this fault system. In addition, considering the long-term slip rates and horizontal offset in previous studies, the recurrence time of earthquakes has approximately 302 years for a magnitude greater than 6.0. Finally, these comprehensive analyses explain the implications of seismic hazard evaluation and forecasting of possible next earthquake occurrences in this region.</p>

### Alıntı / Cite

Alkan, H., Öztürk, S., Akkaya, İ., (2023). Analysis of Coulomb Stress Transfer and Earthquake Hazard in the Çaldıran Fault Zone and its Adjacent Region, Journal of Engineering Sciences and Design, 11(2), 519-534.

### Yazar Kimliği / Author ID (ORCID Number)

H.Alkan, 0000-0003-3912-7503  
S. Öztürk, 0000-0003-1322-5164  
İ. Akkaya, 0000-0002-7682-962X

### Makale Süreci / Article Process

Başvuru Tarihi / Submission Date	28.10.2022
Revizyon Tarihi / Revision Date	26.12.2022
Kabul Tarihi / Accepted Date	05.01.2023
Yayın Tarihi / Published Date	28.06.2023

\* İlgili yazar / Corresponding author: hamdialkan@yyu.edu.tr, +90-432-444-5065

## ANALYSIS OF COULOMB STRESS TRANSFER AND EARTHQUAKE HAZARD IN THE ÇALDIRAN FAULT ZONE AND ITS ADJACENT REGION

Hamdi ALKAN<sup>1†\*</sup>, Serkan ÖZTÜRK<sup>2</sup>, İsmail AKKAYA<sup>1</sup>

<sup>1</sup>Van Yüzüncü Yıl Üniversitesi, Mühendislik Fakültesi, Jeofizik Mühendisliği Bölümü, Van, Türkiye

<sup>2</sup>Gümüşhane Üniversitesi, Mühendislik ve Doğa Bilimleri Fakültesi, Jeofizik Mühendisliği Bölümü, Gümüşhane, Türkiye

### Highlights

- Coulomb stress variations in the Çaldıran fault zone are modeled.
- The small  $b$ -values are observed in the eastern part of Lake Van region.
- The comprehensive analyses show the high seismic hazard potential soon.

### Graphical Abstract

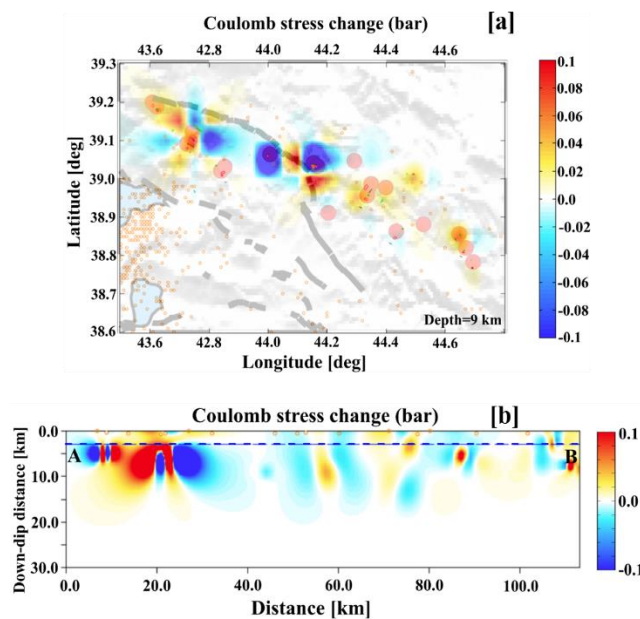


**Figure.** (A) The Same As Figure 7 But At A Depth Of 9 Km (B) The Cross-Section Shown In Figure 7a Is Obtained For A Depth Range Of 0-30 Km.

### Purpose and Scope

The purpose of this study is to investigate the Coulomb stress changes and the earthquake hazard potential.

### Design/methodology/approach

Based on the seismotectonic  $b$ -value, earthquake probability, recurrence times and Coulomb stress changes, the future earthquake potential and positive/negative stress changes are investigated in the Çaldıran fault zone.

### Findings

The regions with small  $b$ -values cover the Çaldıran fault zone, Hasantimur fault, Dorutay fault and Saray fault zone, while high  $b$ -values are detected in the Erciş fault zone. Besides, the high positive Coulomb stress variations using the events that occurred after 2010 are observed in the NW of the Çaldıran fault zone.

### Originality

In this study, we have studied the current earthquake potential in and around the Çaldıran fault zone. For this scope, small earthquakes ( $M_w \leq 4.2$ ) with no focal mechanism solution are selected in the region. After that, fault plane solutions of other events are obtained using SEISAN software. On the other hand, the homogeneous duration magnitude ( $M_d$ ) catalog is used to estimate the parameters of next seismic activity in the region.

<sup>†</sup> Corresponding author: hamdialkan@yyu.edu.tr, +90-432-444-5065

## 1. Introduction

Anatolia is the most seismically active region in the Alpine-Himalayan orogenic system. The tectonic structure of Anatolia is especially due to the relative motion among the Arabian plate, African plate and Eurasian plate (Figure 1). Concerning these relative plate movements, the African oceanic plate moved to the north-northeast direction, started the Early Miocene, and roll-back beneath the western Anatolian along the Aegean-Cyprian arc (Bozkurt, 2001; Reilinger et al., 2006; Ozer et al., 2019). On the other hand, the northward motion of the Arabian plate ( $\sim 15 \text{ mm yr}^{-1}$ ) and southward motion of the Eurasian plate cause a compression mechanism along the Bitlis-Zagros suture (BZS), creating the East Anatolian plateau (EAP) (Delph et al., 2015). This collision started Mid-Miocene time ( $\sim 12 \text{ Ma}$ ) has resulted in the uplift of mountains (up to 2 km) along the suture and caused westward motion and rotation of the Anatolian micro-plate ( $\sim 20 \text{ mm yr}^{-1}$ ), initiated in the Early Pliocene ( $\sim 5 \text{ Ma}$ ), along with the two best-known strike-slip fault systems due to the remarkable seismic activity. The right-lateral North Anatolian fault zone (NAFZ) has a  $24 \pm 2 \text{ mm yr}^{-1}$  motion and the left-lateral East Anatolian fault zone (EAFZ) has a sinistral motion of  $9 \pm 2 \text{ mm yr}^{-1}$ , conjugating near the Karlıova region. On the other hand, the north of the NAFZ is bounded by a Southern Black Sea Thrust Zone, associated with thrusting faults (Yiğitbaş et al., 2004). In the recent tectonic process in the region, the crustal deformation is ongoing and the N-S compressional tectonic regime causes some important thrust/reverse, normal and strike-slip fault mechanisms (McClusky et al., 2000; Bozkurt, 2001; Koçyiğit et al., 2001; Şengör et al., 2003; Tsapanos et al., 2014; Wang et al., 2015; Emre et al., 2018).

The Çaldıran fault zone (CFZ) is the strike-slip fault system in the East Anatolian region (EAR) and is located in the east of the Karlıova triple-junction (KTJ). This fault system has a right-lateral strike-slip mechanism and extends eastward to the North Tabriz fault and westward to Erciş and Tutak faults, considered the southern boundary of the Caucasus block. According to detailed mapping, the CFZ is divided into three individual segments called Gülderen, Hıdırmentes, and Alaçayır sections (Selçuk et al., 2016). The GPS-derived slip rate of this fault system has been studied by different researchers. According to Selçuk et al. (2016), detailed geometry, slip rate and age of the CFZ are insufficient. Djamour et al. (2011) associated this fault zone with the southern boundary of the Lesser Caucasian-Talesh block, moving towards NNE at a velocity of around  $8.3 \text{ yr}^{-1}$ . Also, Copley and Jackson (2006) calculated the GPS-derived slip rate value as  $8 \pm 2 \text{ yr}^{-1}$ . On the other hand, using block modeling, Reilinger et al. (2016) estimated a high slip rate of  $10.1 \pm 1 \text{ yr}^{-1}$  for the CFZ. The CFZ caused many destructive earthquakes in the instrumental and historical periods. According to the earthquake catalog (URL-1) of the Disaster and Emergency Management Authority (AFAD), the region experienced many devastating earthquakes in different years such as 1647, 1664, 1779, 1818 and 1872 around the Tabriz and Van settlements. The last of these devastating earthquakes occurred on 24 November 1976 Çaldıran ( $M_s = 7.3$ ) with an approximately 55 km-long surface rupture (Şaroğlu, 1986; Koçyiğit et al., 2001; Ambraseys, 2009; Utkucu et al., 2013; Selçuk et al., 2016; Emre et al., 2018; Alkan and Akkaya, 2021). This earthquake is one of the biggest earthquakes in the EAR. Quaternary alluvial units consisting of unconsolidated sediments and Pliocene volcanic rocks (trachyte, andesite, and basalts) are common geological units of the Çaldıran fault zone and its surrounding regions (Şaroğlu and Yılmaz, 1986). Thus, in recent years, moderate-size earthquakes continue to occur in the region.

Regarding the previous seismicity, many strong earthquakes were experienced frequently in the region, causing heavy damage in the towns and villages. These destructive events in the past are a view for future large earthquakes. Based on these past events, the main purpose of this study is to explore and understand the different viewpoints for possible future earthquake forecasting and hazard evaluation by performing *b*-value distribution, earthquake probability, recurrence time and Coulomb stress changes in the CFZ. Based on the Coulomb stress analysis at the different depths, we discuss the stress transfer effects of the previous large 1976 Çaldıran earthquake ( $M_s = 7.3$ ) and past earthquakes that occurred along the CFZ between 2010 and 2021 ( $M \geq 3.6$ ), meanwhile, we predict the next potential earthquakes using the homogeneous database for *duration magnitude* ( $M_d$ ) containing the events between 1975 and 2021. In the present study, the Coulomb stress changes of earthquakes that occurred on the CFZ are interpreted with seismotectonic parameters, and the direction of stress transfer is estimated for possible large earthquakes. The combination of these statistical parameters gives significant evidence to forecast earthquakes and detect the time occurrences of future events in real-time for CFZ and its surrounding region.

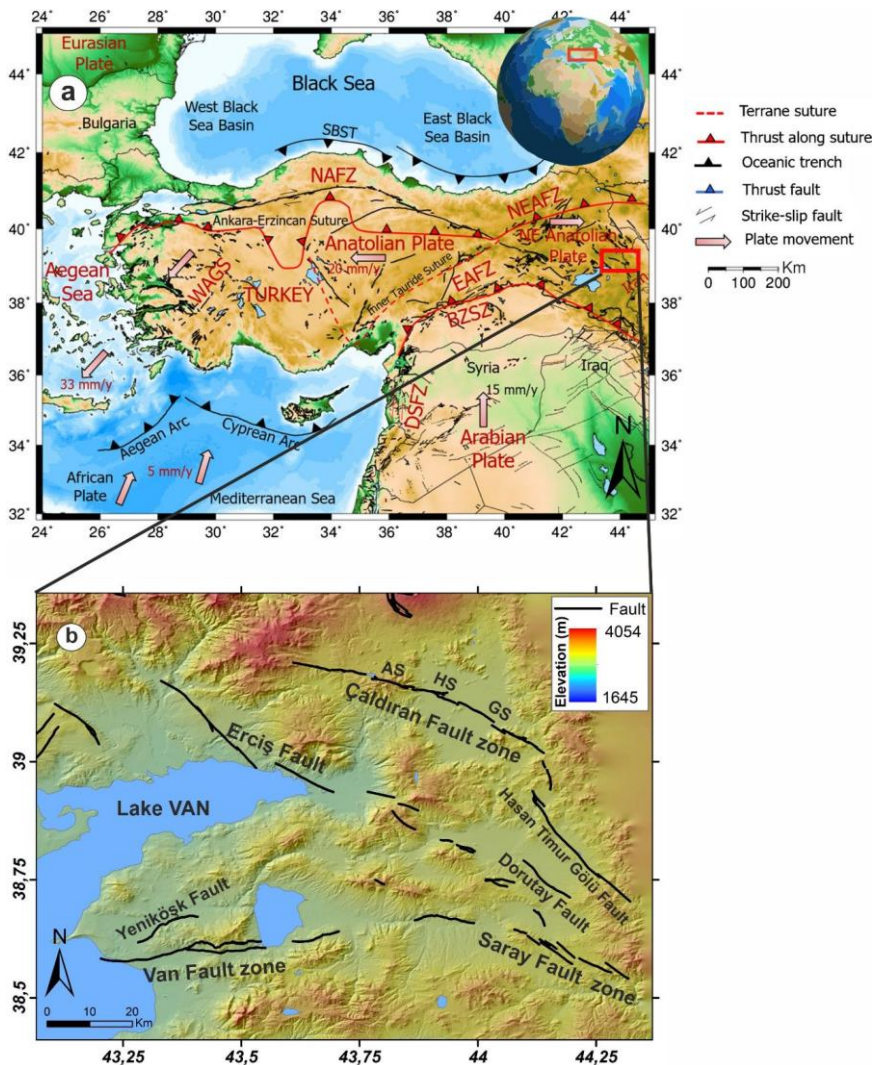


**Figure 1.** (A) The Main Tectonic Elements In And Around Turkey (Modified From Alkan Et Al., 2021). The Study Region Is Shown In A Red Rectangular Frame. The Arrows Depict The Relative Direction Of Plate Motions And Velocities (Reilinger Et Al., 2006) (B) The Morphology Of The Study Region. The Active Tectonic Faults Have Been Taken From Emre Et Al. (2018). Abbreviations: WAGS: West Anatolian Graben System; SBST: Southern Black Sea Thrust; EAFZ: East Anatolian Fault Zone; NAFZ: North Anatolian Fault Zone; NEAFZ, Northeast Anatolian Fault Zone; BZSZ: Bitlis-Zagros Suture Zone; DSFZ: Dead Sea Fault Zone; AS: Alaçayır Segment; HS: Hıdırmenteş Segment; GS: Gülderen Segment

## 2. Methods

### 2.1. Gutenberg-Richter Relation, Recurrence Time And Earthquake Probability

The power-law relation of earthquake distributions is given by Gutenberg and Richter (1944) and this well-known statistic (G-R) is one of the most frequently used forms in seismology. G-R size-scaling relation explains the magnitude-frequency variations of earthquake distributions and this form is given by a mathematical equation as follows:

$$\log_{10} N(M) = a - bM \tag{1}$$

where  $N(M)$  is the cumulative number of earthquakes during a specific time period with magnitudes larger than or equal to  $M$ , whereas the  $a$ -value and  $b$ -value are positive constants. Variations in  $a$ -value are associated with the time interval of the catalog, the size of the study region and the number of earthquakes. Thus, the  $a$ -value shows important changes depending on the seismicity of different regions.  $b$ -value is estimated from the slope of the G-R relation and this parameter is very important to give the characterization of earthquakes. It is stated that the  $b$ -value is associated with the relative number of earthquakes. Many factors such as the tectonic features, anisotropic structure and stress heterogeneities affect the  $b$ -value changes. A negative relationship can be seen between the  $b$ -value and stress distribution. In addition, crack density, geological complexity, material properties, thermal gradient, fault length, strain circumstances, seismic wave velocity changes and attenuation, and slip distribution

lead to variations in the  $b$ -value (Mogi, 1962; Scholz, 2015). The  $b$ -value is changed between 0.3 and 2.0 for different regions in the world (Utsu, 1971). However, the  $b$ -value is defined as around 1.0 on average (Frohlich and Davis, 1993). Thus, previous studies indicate that the  $b$ -value is one of the most significant parameters for the rheological analysis of the region. Earthquake probabilities of different magnitude sizes can be calculated from the next equation (Ali, 2016):

$$P(M) = 1 - e^{-N(M)*Tr} \quad (2)$$

where  $P(M)$  is the probability that an event occurs in given  $Tr$  years.  $N(M)$  and  $M$  are derived from Equation 1. On the other hand, the recurrence times for different magnitudes can be calculated from the formula (Ali, 2016):

$$Q = 1 / N(M) \quad (3)$$

where  $Q$  is the recurrence time and is defined as the expected time interval for an earthquake with a magnitude greater than or equal to  $M$ . Magnitude completeness ( $Mc$ -value) is the other important parameter in the statistical analysis.  $Mc$ -value is the minimum magnitude and can be estimated from the magnitude-frequency distribution (Wiemer and Wyss, 2000). This magnitude level encompasses 90% of the earthquakes in the catalog. Temporary differences in the  $Mc$ -value can influence the seismicity parameters such as the  $b$ -value. Thus, the maximum earthquake numbers are planned to be used for exact results for the analysis. Therefore, this type of estimation must be considered in the first stage of the analysis. In this study, some of the statistical parameters are calculated by using the *ZMAP* package introduced by Wiemer (2001).

## 2.2. Coulomb Stress Change

The Coulomb failure stress change ( $\Delta\sigma_{cfs}$ ) for a source fault is given by the difference between the shear stress change ( $\Delta\tau_s$ ) which is positive in the direction of slip and the effective normal stress change ( $\Delta\sigma_n$ ) along the fault plane and the effective coefficient of friction ( $\mu'$ ) changed within 0 to 1, as follows:

$$\Delta\sigma_{cfs} = \Delta\tau_s + \mu' \Delta\sigma_n \quad (4)$$

The effective coefficient of friction is regarded as 0.4 in an elastic half-space and included changes in pore pressure (King et al., 1994). Young's modulus ( $E$ ) is selected as  $8 \times 10^5$  bars and Poisson's ratio ( $\nu$ ) is 0.25 for this study. The Coulomb stress observation between -0.1 and 0.1 (bar) is satisfactory to forecast following earthquake hazards (Yadav et al., 2012). The increased Coulomb stress variation represents the loading stress, pushing the fault toward brittle failure, while the declined Coulomb stress change corresponds to the unloading stress, inhibiting earthquake rupture (Stein et al., 1994). In this study,  $\Delta\sigma_{cfs}$  changes are obtained with the Coulomb 3.4 software (Toda et al., 2011). The source parameters for all earthquakes are used to calculate  $\Delta\sigma_{cfs}$ , showing generally strike-slip fault mechanisms.

## 3. Data

For the statistical analysis, a part of the homogeneous *duration magnitude* ( $M_d$ ) catalog is obtained from Öztürk (2009) (for details see Bayrak et al., 2009), which is composed of 83 events between 1970 and 2006. The other catalog, which is existed 6086 events, is supplied by Kandilli Observatory and Earthquake Research Institute (KOERI) between 2006 and 2022. The part of the earthquake database on the KOERI until 2012 shows that the given magnitude type is  $M_d$ . After 2012, the catalog gradually starts to transform into *local magnitude* ( $M_L$ ). Therefore, instead of converting a 40-year  $M_d$  type to the last 10-year  $M_L$  type, it has been deemed more appropriate to use the data for the last 10 years of empirical  $M_d - M_L$  relations. KOERI provides the *local magnitudes* of the earthquakes for  $M_d$  which is not calculated recently. In this status where  $M_d$  was not determined in the KOERI catalog between 2006 and 2022, unknown  $M_d$  is calculated from  $M_d - M_L$  equations suggested by Bayrak et al. (2009). In this way, the errors in the magnitude conversions are further reduced. For this reason, the  $M_d$  type is used instead of the other magnitude types for more reliable results, and magnitudes in the target catalog are not calculated empirically. The shallow earthquakes (depth  $\leq 70.0$  km) are preferred to make the statistical evaluations. Because Alkan et al. (2020) stated that seismogenic depth changes between 40 and 45 km for the East Anatolian region covering the study region. Finally, an earthquake catalog with a magnitude range of  $1.0 \leq M_d \leq 5.6$  including 6169 earthquakes between July 12, 1975, and December 29, 2021, approximately 46.47 years, is prepared. Epicenter locations of the original catalog consisting of 6169 earthquakes are plotted in Figure 2 by using different symbols for different magnitude levels.

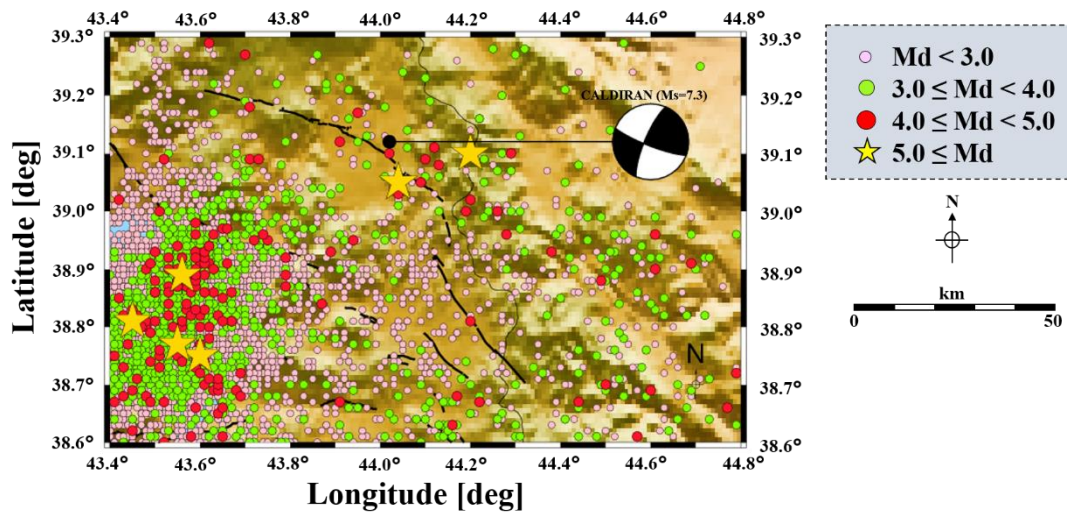


**Figure 2.** Epicenter Distribution Of 6169 Earthquakes From 1975 To 2020. Also, The Çaldıran Earthquake ( $M_S = 7.3$ ) And Its Fault Plane Solution Are Given In The Figure

For the Coulomb failure stress change, source parameters of selected events ( $M \geq 3.6$ ) that occurred along the CFZ between 2010 and 2021 and the 1976 Çaldıran earthquake ( $M_S = 7.3$ ) are given in Table 1. Although the focal mechanism parameters (strike/dip/rake) of some earthquakes (event numbers are 5, 6, 8 and 10) are given by the AFAD, fault plane solutions of other events are obtained using SEISAN software (Ottemöller et al., 2021) with broad-band stations records (Figure 3). In addition, the focal parameters of the 1976 Çaldıran earthquake, which is very important to interpret stress variation in the study region, are taken from the USGS (URL-2). SEISAN is very advantageous computer software and is built on some programs to analyze earthquakes from local and global data. PPFIT (Reasenber and Oppenheimer, 1985) and PINV (Suetsugu, 1998) are integrated into SEISAN software to understand the fault plane mechanism. PPFIT gets the double-couple fault-plane solution using the source model compatible with the study region. PPFIT uses first observing polarities for a suite of earthquakes and gives the inversion results via a two-stage grid search algorithm, which is the weighted sum of first motion polarity discrepancies. The algorithm calculates the uncertainty in the model parameters for the estimated uncertainty interval (Reasenber and Oppenheimer, 1985). On the other hand, PINV (Suetsugu, 1998) gives the best focal mechanism solution depending on P-phase polarities (Ottemöller et al., 2021). Figure 3 demonstrates the focal mechanism solutions and epicenter locations of all events with the spatial distribution of broad-band stations.

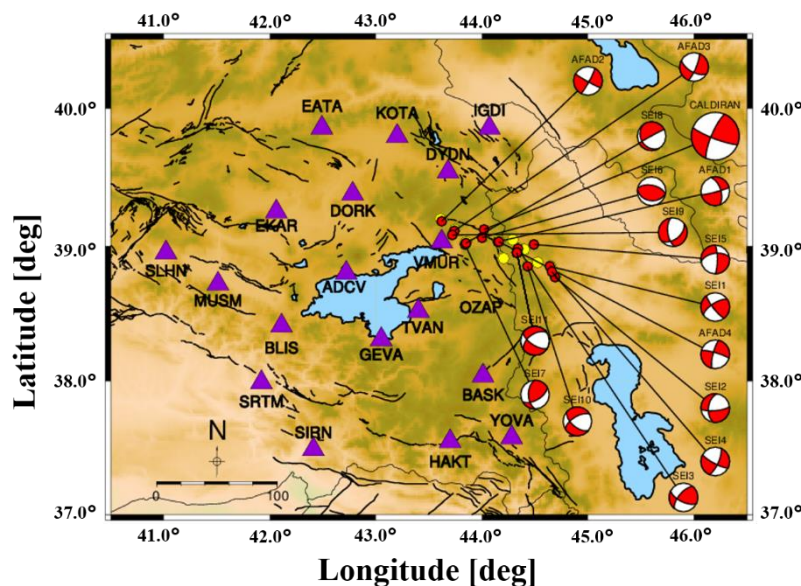


**Figure 3.** The Selected Earthquakes Along With The Çaldıran Fault Zone To Investigate Coulomb Stress Changes. The AFAD And SEI On Each Beach Ball Represent AFAD And SEISAN Focal Mechanism Solutions, Respectively. The Yellow Circles Show Earthquakes With No Broad-Band Station Records. The Purple Triangles Represent The Broad-Band Stations Used For The Focal Mechanism Solutions

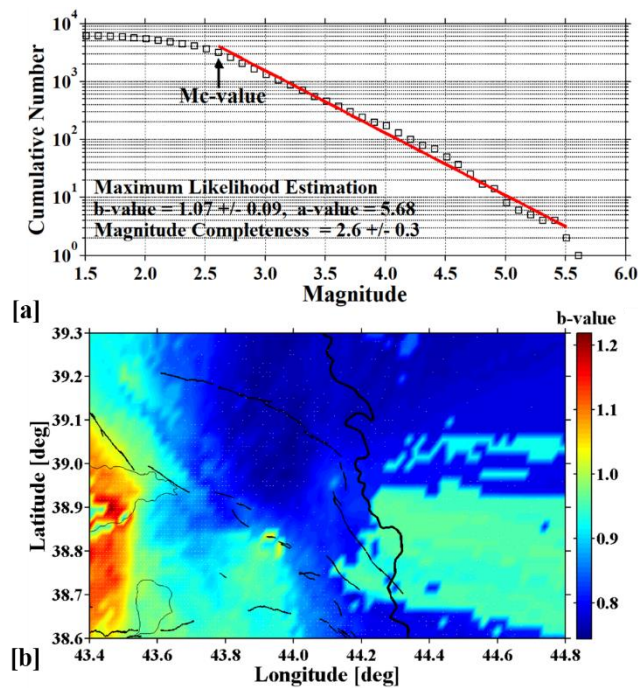
**Table 1.** Focal Parameters Of Earthquakes Obtained From The AFAD (URL-1) And SEISAN Software To Calculate Coulomb Failure Stress Changes In The Study Region

No	Date (dd/mm/yy) (hh:mm:ss)	Depth (km)	Mag	Lat (°N)	Long (°N)	S/D/R (°)	Source
1	22/06/2021 22:43:06	5.24	M <sub>w</sub> =4.2	38.853	44.647	142°/78°/158°	Seisan/FPFIT
2	14/07/2020 09:22:56	7.34	M <sub>i</sub> =3.6	38.779	44.694	85°/75°/-41°	Seisan/FPFIT
3	14/09/2019 15:33:42	11.78	M <sub>w</sub> =4.5	38.984	44.349	220°/64°/29°	Seisan/PINV
4	23/07/2018 11:35:58	2.05	M <sub>w</sub> =3.8	38.816	44.669	118°/78°/-161°	Seisan/FPFIT
5	21/07/2018 06:15:13	7.52	M <sub>w</sub> =4.5	39.038	44.153	75°/85°/-148°	AFAD
6	18/09/2017 09:41:07	4.31	M <sub>w</sub> =4.1	39.186	43.623	119°/86°/-173°	AFAD
7	29/11/2015 06:08:54	7.12	M <sub>w</sub> =3.8	39.017	44.496	0°/78°/-141°	Seisan/FPFIT
8	29/10/2015 09:46:39	4.90	M <sub>w</sub> =4.8	39.119	43.743	119°/61°/-167°	AFAD
9	10/10/2013 03:00:00	9.25	M <sub>i</sub> =3.6	39.061	44.006	97°/34°/86°	Seisan/PINV
10	13/04/2012 00:04:48	4.28	M <sub>i</sub> =4.3	39.030	44.167	286°/81°/-167°	AFAD
11	31/03/2012 12:41:19	4.89	M <sub>i</sub> =3.6	39.018	43.840	60°/58°/134°	Seisan/PINV
12	31/03/2012 10:38:18	4.14	M <sub>i</sub> =3.9	39.029	43.853	147°/25°/-5°	Seisan/PINV
13	09/03/2012 06:14:17	7.0	M <sub>i</sub> =3.9	39.089	43.725	52°/48°/-41°	Seisan/FPFIT
14	06/12/2010 05:16:08	2.4	M <sub>i</sub> =4.1	38.955	44.335	123°/65°/-43°	Seisan/FPFIT
15	06/11/2010 01:05:14	5.0	M <sub>i</sub> =4.1	38.859	44.433	130°/58°/-33°	Seisan/PINV
16	24/11/1976 12:22:18-	36.0	M <sub>s</sub> =7.3	39.121	44.029	111°/81°/167°	USGS

#### 4. Results And Discussion

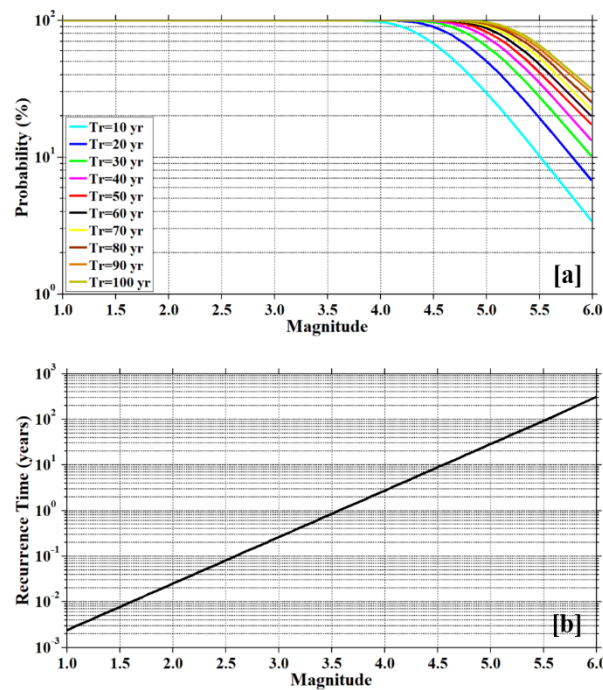
Coulomb stress changes, seismotectonic  $b$ -value, probability and recurrence times are used to understand how earthquakes interact with each other and to predict future seismic hazard. For this purpose, the Coulomb stress variations calculated by the 1976 Çaldıran earthquake and the recent earthquakes are compared at different depth intervals. The obtained stress changes along the CFZ are then contrasted with the  $b$ -value changes, probability and recurrence times of the events.

The  $b$ -value changes, magnitude-frequency distribution, standard deviation,  $a$ -value and  $M_c$ -value are demonstrated in Figure 4. The  $b$ -value is calculated with the maximum likelihood method (Aki, 1965). As indicated in Figure 4a, the average  $M_c$ -value for all catalogs is taken as 2.6 and the  $b$ -value is determined as  $1.07 \pm 0.09$ . As previously mentioned, the  $b$ -values vary between 0.3 and 2.0 on the global scale and tectonic events are presented with a  $b$ -value changing from 0.5 to 1.5 with an average of  $\sim 1.0$ . The regional variation of  $b$ -value is also demonstrated in Figure 4b. The  $b$ -value map is obtained by using a moving window technique with a sample of 1100 earthquakes and prepared by grid cell spacing of  $0.02^\circ$  in longitude and latitude. The regional variation of the  $b$ -value is estimated at 0.75 to 1.21. The regions with the high  $b$ -values ( $> 1.0$ ) are estimated in and around the eastern part of Lake Van including the Erciş fault zone. However, the regions with the low  $b$ -values ( $< 1.0$ ) are observed in all regions including the Çaldıran fault zone consisting of the Alaçayır segment, Hidirmenteş segment and Gülderen segment, Hasantimur fault, Dorutay fault and Saray fault zone. The regions with the small  $b$ -values correspond to great-magnitude earthquakes (Figure 2). Consequently, the  $b$ -value estimation presents the best fit with seismic activity.



**Figure 4.** (A) Magnitude-Frequency Distribution And  $B$ -Value Of G-R Relation.  $B$ -Value, Its Standard Deviation,  $A$ -Value, And  $M_c$ -Value Are Also Supplied In Figure (B) Regional Variations In  $B$ -Value For The Study Region

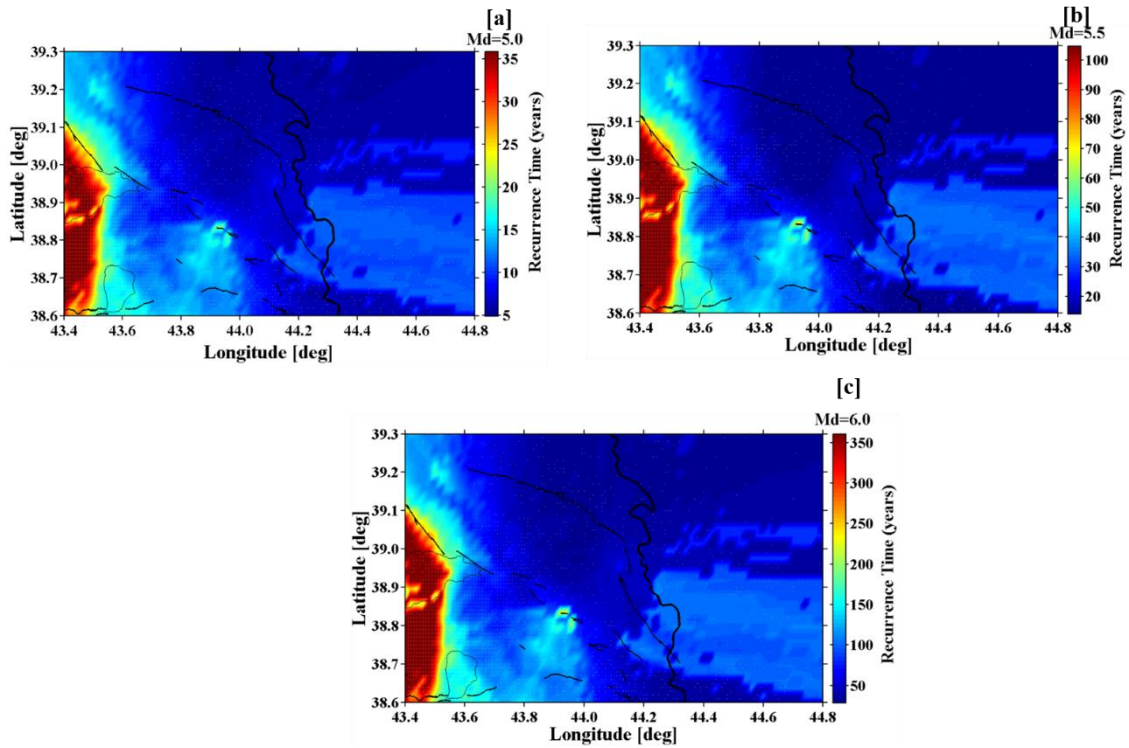
One of the most important applications for statistical behaviors of earthquake occurrence includes the estimation of probabilities and recurrence times. For this purpose, earthquake probabilities and recurrence times of different magnitudes that the catalog includes are drawn in Figure 5. As stated in the data section, the earthquake catalog consists of a magnitude range between 1.0 - 5.6 and the largest magnitude in the earthquake catalog with  $M_d = 5.6$  is the 1976 Çaldıran earthquake. For this reason, the largest earthquake magnitude is chosen as  $M_d = 6.0$  on the magnitude axes. Probabilities of earthquake activity in different magnitudes show comparatively great values changing from 70-100 % for earthquakes of  $1.0 \leq M_d \leq 4.5$  and the values relatively lower than 70 % for earthquakes of  $4.5 \leq M_d$  (Figure 5a). According to Figure 5a, the probabilities of earthquakes with  $M_d = 5.0$  in  $Tr = 10, 20, 50, 70$  and 100 years are estimated as about 30 %, 50 %, 84 %, 92 % and 97 %, respectively. The probabilities of  $M_d = 5.5$  earthquakes in  $Tr = 10, 20, 50, 70$  and 100 years are calculated as about 11 %, 20 %, 44 %, 55 % and 68 %, respectively. Also, the probabilities of  $M_d = 6.0$  earthquake occurrences in  $Tr = 10, 20, 50, 70$  and 100 years are found as about 4 %, 7 %, 18 %, 23 % and 32 %, respectively. Therefore, the probabilities of the other magnitude levels in the other  $Tr$  years can be estimated from Figure 5a. The recurrence times of the earthquakes in different magnitudes are drawn in Figure 5b. Slightly small recurrence times ( $< 1.0$  years) are estimated for the magnitude levels between 1.0 and 3.5. The recurrence times of 1 to 10 years are calculated from 3.5 to 4.5 magnitude intervals. Also, the recurrence times of 10 to 100 years can be anticipated for the magnitude interval between 4.5 and 5.5, while the recurrence times bigger than 100 years can be regarded as magnitudes larger than 5.5. As seen in Figure 5b, the recurrence times of  $M_d = 5.0, 5.5$  and 6.0 earthquakes are estimated as about 29, 90 and 300 years, respectively. Also, the recurrence times of the other magnitude levels can be easily observed in Figure 5b. The results of probabilities and recurrence times suggest that earthquake occurrences changing from 3.0 - 4.5 magnitude levels are more probable than those of the other occurrences in the short term. Thus, these results can supply usable findings to define the statistical behaviors of strong earthquake occurrences in the study region.



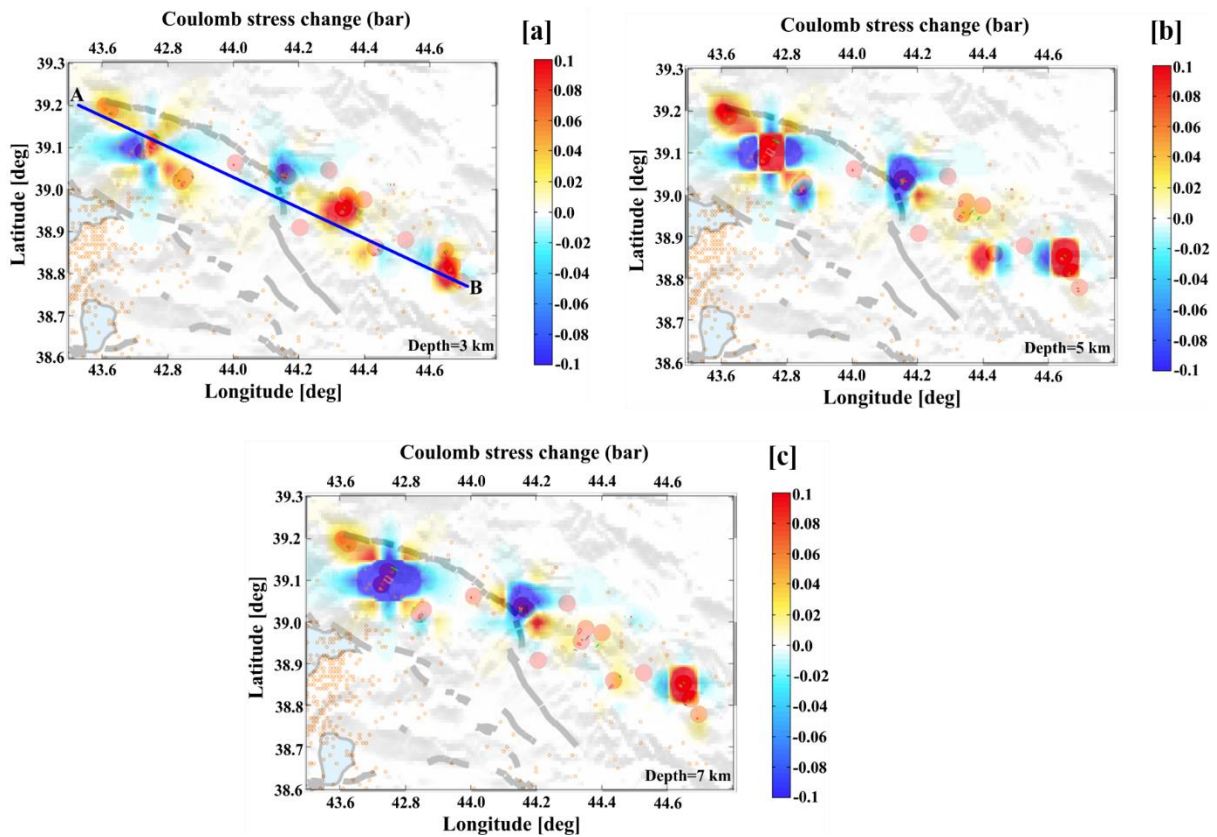
**Figure 5.** (A) Probability Of Earthquakes That A Given Magnitude Will Be Exceeded In Specific Times  $Tr = 10, 20, 30, 40, 50, 60, 70, 80, 90$  And  $100$  Years (B) Recurrence Times For Different Magnitude Levels Of The Earthquake Occurrences

Recurrence time change for the events with  $M_d = 5.0, 5.5$  and  $6.0$  are plotted in Figure 6. As given in Figure 6a, recurrence times are estimated as relatively smaller, ranging between 5 and 35 years, for a magnitude level of  $M_d = 5.0$ . Recurrence times changing 25 to 35 years are estimated in and around the eastern part of Lake Van including the Erciş fault. The other regions have small recurrence times ( $\sim 15$  years) for the  $M_d = 5.0$ . Figure 6b depicts the recurrence times of  $M_d = 5.5$  earthquakes, ranging from 20 to 100 years. Also, recurrence times of  $M_d = 6.0$  magnitude are drawn in Figure 6c. Recurrence times for this magnitude size vary generally from 50 to 350 years. As seen from Figures 6a, 6b and 6c, the regions with smaller/greater recurrence times are estimated in nearly the same regions. This means that there is a good relationship between the  $b$ -value and recurrence time. As seen from Figure 6, recurrence times for strong earthquakes with  $M_d = 5.0$  are roughly between 5 and 15 years for a large part of the study region. This result can be promoted by recurrence times with magnitude shown in Figure 5. The detailed analysis of recurrence times for strong earthquake occurrences shows an earthquake potential in the intermediate/long term. Therefore, these earthquake behaviors can promote earthquake hazard in the future.

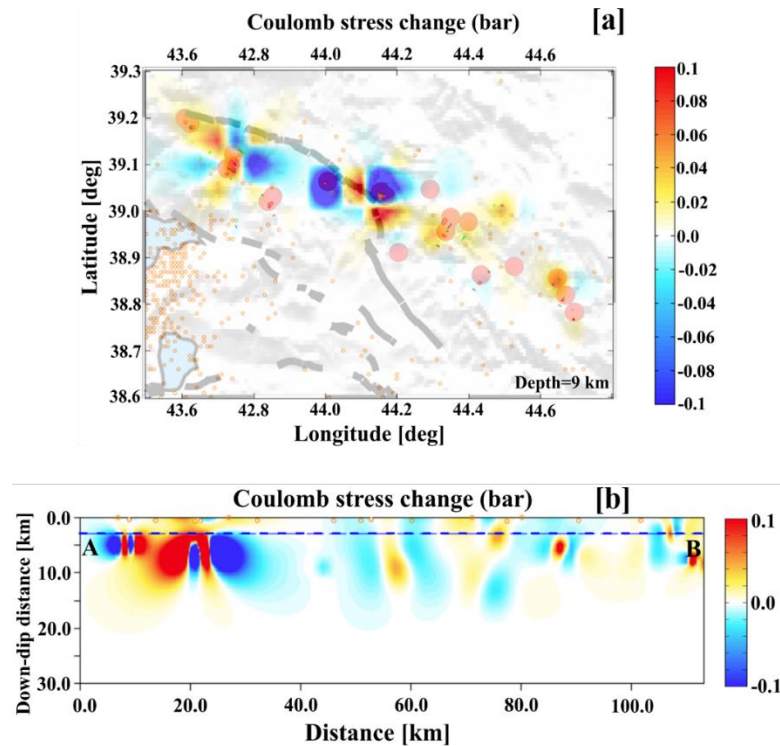
Figures 7 and 8 demonstrate the Coulomb stress variations at a depth of 3, 5, 7 and 9 km around the main rupture of CFZ. The chosen depth ranges to observe stress changes are associated with the hypocenter depths of the selected earthquakes. In the Coulomb stress change maps, the warm colors indicate positive stress values (bar) while the cold colors represent negative stress values (bar). Since the fault mechanism solutions of selected events reflect optimally oriented strike-slip fault mechanisms (Figure 7), the stress variations are calculated into this fault mechanism. In Figures 7 and 8, we observe clustered and small-scale stress variations for each depth level. Especially at shallow depths, the stress changes are positive values towards the North Tabriz fault in the SE direction, whilst it is observed that the stress is positive values at the northwest section of the CFZ at a depth of 5 km. On the other hand, the cross-section "A-B" passes through the hypocentral locations of earthquakes to observe the vertical stress changes as shown in Figure 7a. Along with the "A-B" profile in an NW-SE direction, there is a positive-stress region observed up to 10 km depth in the northwest segment of the CFZ called Alaçayır. However, the stress level towards the southeast is observed at really low values at all depth levels. Besides, it can be observed that the stress is quite low at increasing depths due to the hypocentral distribution of earthquakes.



**Figure 6.** Regional Variations Of The Recurrence Times For Selected Magnitude Levels Including Strong/Large Earthquakes: (A)  $M_d = 5.0$ , (B)  $M_d = 5.5$  And (C)  $M_d = 6.0$



**Figure 7.** Coulomb Stress Changes Are Produced By The Earthquakes Shown In Table 1 Except For The Çaldıran Mainshock At A Depth Of 3 Km (A), 5 Km (B) And 7 Km (C). The Solid Blue Line (A-B) In (A) Shows The Vertical Cross-Section Profile. The Red Circles Demonstrate The Locations Of The Earthquakes (Source Parameters Are Listed In Table 1). The Small Pink Circles Show Earthquakes That Occurred After 2000 In The Study Region (URL-3). Thick Black Lines Represent Active Faults In The Study Region (Modified From Emre Et Al., 2018).



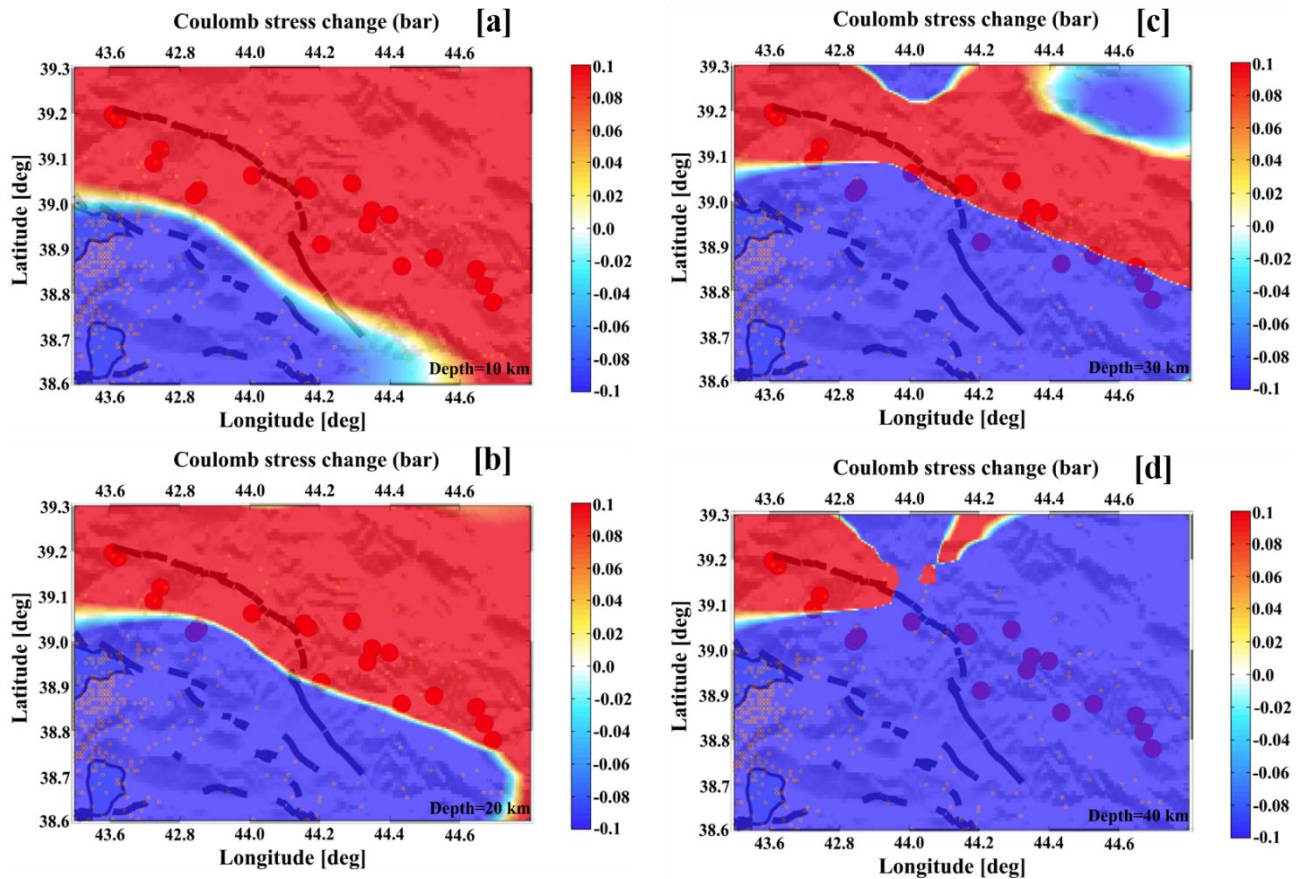
**Figure 8.** (A) The Same As Figure 7 But At A Depth Of 9 Km (B) The Cross-Section Shown In Figure 7a Is Obtained For A Depth Range Of 0-30 Km

Figure 9 shows the Coulomb stress changes related to the occurrence of the 1976 Çaldıran mainshock ( $M_s = 7.3$ ) for a depth of 10 to 40 km. The focal parameter solution of USGS shows a dextral strike-slip fault with ( $111^\circ$  strike,  $81^\circ$  deep and  $167^\circ$  rake) with 50 - 55 km surface rupture (Selçuk et al., 2016; URL-2). This devastating earthquake created high positive stress values at depths of 10, 20 and 30 km depth in the region. It is demonstrated that the study region is divided into two lobes along the Çaldıran fault zone. Positive-stress values in the north-northwest trend (red) and negative-stress values in the south-southeast trend (blue) can be observed clearly for 10 to 30 km depth intervals. Coulomb stress variation maps (Figures 7 and 8), calculated by using earthquakes that occurred after 2010 (Table 1), demonstrate that there is a higher stress accumulation around the NW segment of the CFZ, Alaçayır segment, despite having shallow focal depths ( $\sim 10$  km). The positive stress region appearing on the Coulomb stress change maps of the 1976 Çaldıran mainshock is also directly related to this vicinity of the Çaldıran fault zone. On the other hand, as shown in Figures 9 and 10, the epicenter locations of the earthquakes selected after 2010 are within the positive stress region calculated from the 1976 mainshock. Concerning the shallow earthquake-generating mechanism of the EAR, the positive stress change region obtained from the 1976 main shock provides the consistency of these study results. However, up to 40 km depth, stress change is accumulated in the northwest direction of CFZ (Alaçayır segment), whilst negative stress values are observed in the Hıdırmentes segment and the Gülderren segment. This high-stress change proves that the stress transfer is along with the Alaçayır segment in the northwest direction. Also, it reduces the likelihood of an earthquake occurring at increasing depths southeast of the CFZ, Hıdırmentes, and Gülderren segments. In this case, finally, the stress transfer of the CFZ may be towards the Erciş fault and Tutak fault in the northwest direction.

There exist numerous analyses including different seismic and tectonic parameters to make comprehensive assessments of the future seismic potential in the East Anatolian region. The general interest in the Van Lake region is quite high after the 2011 Van earthquake. For this reason, many studies are performed to provide regional seismic hazards (Öztürk, 2009; Irmak et al., 2012; Bayrak et al., 2013; Elliot et al., 2013; Tsapanos et al., 2014; Öztürk, 2015). However, although the Çaldıran fault zone is an important mechanism due to seismic potential concerning occurrences of strong earthquakes, the number of previous studies is quite limited.

Irmak et al. (2012) studied the main rupture process of the 2011 Van earthquake ( $M_w = 7.1$ ), extending an N-S direction from Erciş to Van. The focal mechanism solution of the mainshock was accompanied by the main thrust fault in direction of NE-SW. The main shock and secondary structural elements such as left-lateral strike-slip faults and intra-plate tensional cracks were generated by the continental-continental plate collision in the region. Irmak et al. (2012) stated that these secondary structural elements caused very probable great earthquakes, especially in the NE direction beyond the mainshock. Akıncı and Antonioli (2013) investigated the effect of big and possible earthquakes in the Lake Van region. The stress redistribution computation of Akıncı and Antonioli (2013)

demonstrated that the Coulomb stress changes were positive in the Lake Van region and the stress level was enhanced in the northern CFZ. Toker et al. (2021) created off-fault-stress modeling of the crustal depths using the 2011 Van earthquake and aftershocks. They suggested that mainshocks and aftershocks increased the intensity of the stress field in an off-fault region through the upper or brittle crust, the SW-NE direction of the source rupture. Consequently, the results of the Coulomb stress variations in the present study are compatible with those of Irmak et al. (2012), Akıncı and Antonioli (2013) and Toker et al. (2021).



**Figure 9.** Coulomb Stress Changes Are Produced By The 1976 Çaldıran Mainshock ( $M_s = 7.3$ ) At A Depth Of 10 Km (A), 20 Km (B), 30 Km (C) And 40 Km (D). The Red Circles Demonstrate The Locations Of The Selected Earthquakes. The Pink Circles Show Earthquakes That Occurred After 2000 In The Study Region (URL-3). Thick Black Lines Represent Active Faults In The Study Region (Modified From Emre Et Al., 2018).

Öztürk (2018) revealed the current earthquake potential in the Eastern Anatolia region of Turkey. According to the fractal dimension ( $D_c$ ) value,  $b$ -value, and the seismic quiescence  $Z$ -value, the CFZ and its surroundings reflected low  $b$ -values ( $\leq 1.0$ ) and were characterized by high-magnitude earthquakes.  $D_c$ -values were calculated as bigger than 2.2, associated with high-stress values. Also, Öztürk (2017) calculated that the recurrence times of earthquake occurrences for magnitudes greater than 6.0 was approximately 10 years for the EAR which held an earthquake hazard potential. On the other hand, Alkan and Bayrak (2021) investigated tectonic Coulomb stress variations and  $b$ -values distribution of the Lake Van region. In the study of Alkan and Bayrak (2021), the earthquakes that occurred in the Lake Van region were used to calculate the Coulomb stress changes. These local event selections gave the stress change topically and showed negative stress changes towards the SW of the Çaldıran fault zone. These previous results are compatible with the stress change maps of the 1976 Çaldıran earthquake (Figure 9) given the negative stress values towards the south of the Çaldıran fault zone at crustal depths. Besides, Alkan and Bayrak (2021) obtained  $b$ -values smaller than 1.0 around the CFZ. This value was in accord with the higher stress release around the southern part of CFZ.

Utkucu et al. (2013) analyzed Coulomb stress variations concerning the 2011 Van earthquake. They suggested that the 1976 Çaldıran earthquake ( $M_s = 7.3$ ) was a recurrence of the 1696 Çaldıran earthquake ( $M_s = 6.8$ ). Also, the 1976 Çaldıran earthquake caused an increase in stress over the 2011 Van earthquake. They defined four aftershock distribution clusters regarding the 2011 Van earthquake and there was stress transfer towards the CFZ in the direction of NE. Also, Reilinger et al. (2006), Copley and Jackson (2006), and Djamour et al. (2011) calculated the GPS-derived slip rate for the CFZ. According to their findings, the long-term slip rates based on the large

earthquake ( $M \geq 6.0$ ) recurrence time are 231, 343 and 331 years, respectively. According to the results of the present study, the recurrence time of a strong earthquake ( $M \geq 6.0$ ) is approximately 300 years. In addition to that, Figure 10 shows the instrumental and historical periods of seismic activity. In the region, the average return period for an event with a magnitude of  $M_w \geq 7.0$  /  $I = \sim 8.0$  is  $\sim 100$  yr, especially after the 16th century. The destructive earthquakes occurred in the SE-NW direction between the Çaldıran fault zone and the North Tabriz fault zone. This recurrent seismicity is most probably associated with these fault zones. Therefore, the findings of this study about the recurrence times are similar to the findings of Utkucu et al. (2013) and these results can be useful for the earthquake hazard evaluation in the intermediate/long term for the study region.

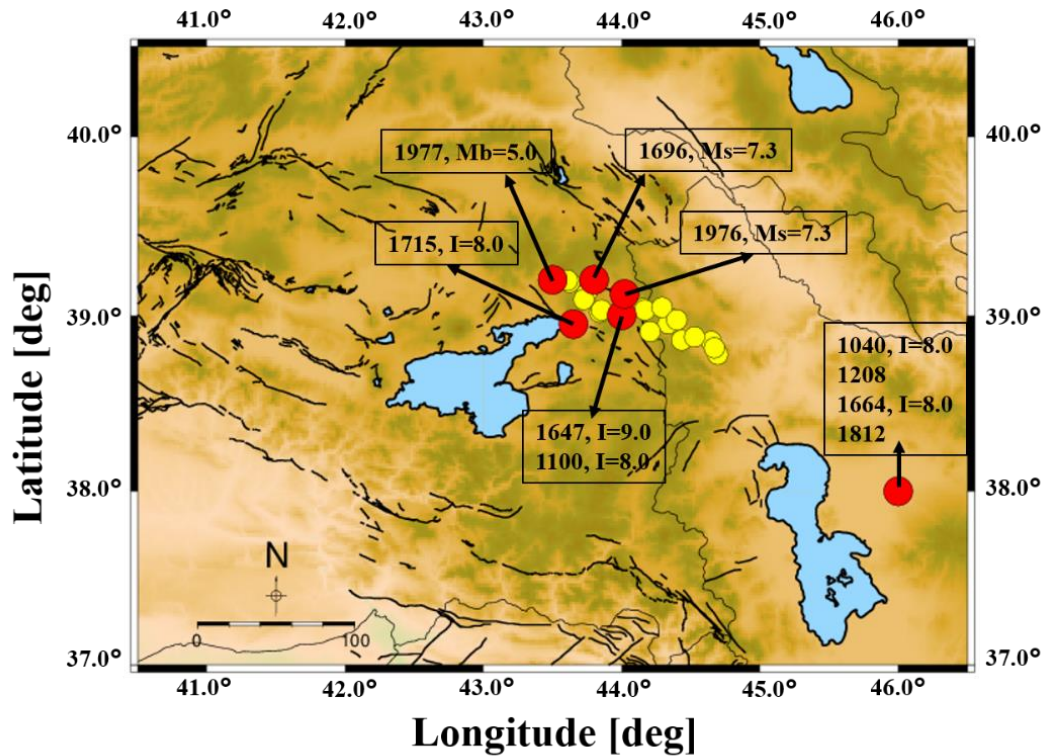


**Figure 10.** Instrumental And Historical Period Seismicity Of The Study Region. The Symbol "I" Depicts Earthquake Intensity. Large Red Circles Indicate Devastating Earthquakes That Have Occurred In The Region (Utkucu Et Al., 2013; URL-1). Yellow Circles Show The Earthquakes (Source Parameters Are Listed In Table 1) That Occurred After The 1976 Çaldıran Mainshock And Are Used To Calculate The Coulomb Stress Change Along With The CFZ.

The general tectonic compression regime (N-S direction), the existence of fault mechanisms (thrust and strike-slip faults) (Mackenzie et al., 2016), the slip models resolved by InSAR observations (Elliott et al., 2013), recent earthquake activities (2011 Van earthquake ( $M_w = 7.1$ ), 2011 Edremit earthquake ( $M_w = 5.6$ ), 2020 Khoy earthquakes ( $M_w = 5.9$  and  $6.0$ ), and 2020 Saray earthquake ( $M_w = 5.4$ )) and Coulomb stress variations show that the earthquake generation potential of the northern parts of the Lake Van region has increased. Considering the changes in the  $b$ -value and Coulomb stress variation, CFZ contains high seismic risk. On the other hand, CFZ has not produced a major or devastating earthquake since 1976 and it is associated with the North Tabriz fault. These are the other important seismic risk factor for the region. In addition to this, the deficiency of earthquake seismic stations in the region and the limited digital data increase the importance of the results of this study.

Another extremely important output obtained from this study is the relationship between the statistical parameters and the building stock in the region. The shallow earthquake potential (Mackenzie et al., 2016), the local geological units, and the low-building quality (Alkan and Akkaya, 2021) may cause high acceleration, an increased probability of damage, and a high seismic hazard. Considering the loss of life and damage after the 1976 Çaldıran earthquake, the population and building density compared to today have increased by 1-1.5 million in the surrounding provinces. On the other hand, the building stock has changed dramatically. When imagining an earthquake similar to the 1976 Çaldıran mainshock, the possible loss of life and property will inevitably be higher than the damage at that time.

## 5. Conclusion

In the current study, seismotectonic  $b$ -value, earthquake probability and recurrence times with Coulomb stress changes are taken into consideration for a reliable seismic hazard and forecasting of strong earthquakes in and around the Çaldıran fault zone. For this purpose, we use a homogeneous catalog composed of 6169 shallow events (depth  $\leq 70.0$  km) with  $1.0 \leq M_d \leq 5.6$  from July 1975 to December 2021. The statistical analyses are performed in the region covered by coordinates  $38.6^\circ N - 39.3^\circ N$  and  $43.4^\circ E - 44.8^\circ E$ . For the mapping of Coulomb stress changes, 15 events with  $M \geq 3.6$  that occurred in and around the Çaldıran fault zone between 2010 and 2021 and the 1976 Çaldıran mainshock ( $M_s = 7.3$ ) are used. These seismotectonic parameters are applied to predict future earthquake occurrences. The regions with small  $b$ -values ( $< 1.0$ ) cover the Çaldıran fault zone, Hasantimur fault, Dorutay fault and Saray fault zone, while high  $b$ -values ( $> 1.0$ ) are detected in the Erciş fault zone. Besides, the high positive Coulomb stress variations ( $\sim 0.1$  bar) using the events that occurred after 2010 are observed in the NW of the Çaldıran fault zone. However, in other segments of the CFZ, the derived  $\Delta\sigma_{cfs}$  values are more complex. As an important note, the Coulomb stress variation of the 1976 Çaldıran earthquake shows the high in the N-NE region of the CFZ, especially at shadow depths. It is well known that a region with small  $b$ -value, high-stress variations and historical seismic activity is indicated to be the future strong/large earthquake region. In addition to this, the evidence from earthquake probabilities and recurrence times exhibits that the occurrence of earthquakes with a magnitude less than 4.5 in the short term is a high probability and the anomalies of strong earthquakes ( $M \geq 6.0$ ) are also quite compatible with the recurrence times of previous large earthquakes. Finally, the findings of the present study can interpret a great guide for further seismic hazard studies in near future.

### Acknowledgments

Firstly, we thank Editor and reviewers for constructive comments and suggestions. After that, the digital seismic waveforms were retrieved from the Disaster and Emergency Management Authority (<https://deprem.afad.gov.tr/>). Next, Coulomb stress changes were calculated *Coulomb 3.4* software (Toda et al., 2011). Also, Some figures are drawn using *Generic Mapping Tools* (Wessel et al., 2013).

### Conflict of Interest

No conflict of interest was declared by the authors.

### References

- Ali, S.M., 2016. Statistical analysis of seismicity in Egypt and its surroundings. *Arab. J. Geosci.*, 9, 52.
- Ambraseys, N.N., 2009. *Earthquakes in the Mediterranean and Middle East*, Cambridge University Press, New York.
- Bayrak, Y., Öztürk, S., Çınar, H., Kalafat, D., Tsapanos, T., Koravos, G.-Ch., Leventakis, G.A., 2009. Estimating earthquake hazard parameters from instrumental data for different regions in and around Turkey. *Eng. Geol.*, 105, 200-210.
- Akinci, A., Antonioli, A., 2013. Observations and stochastic modelling of strong ground motions for the 2011 October 23 Mw 7.1 Van, Turkey, earthquake. *Geophys. J. Int.*, 192, 1217-1239.
- Alkan, H., Çınar, H., Oreshin, S., 2020. Lake Van (southeastern Turkey) experiment: Receiver function analyses of lithospheric structure from teleseismic observations. *Pure Appl. Geophys.*, 177, 3891-3909.
- Alkan, A., Akkaya, İ., 2021. Investigation of Çaldıran (Van) Settlement Area Under the Effect of Active Tectonics by Surface Wave Methods. *Bitlis Eren University Journal of Science*, 10 (4), 1435-1447.
- Alkan, H., Bayrak, E., 2021. Coulomb Stress Changes and Magnitude-Frequency Distribution for Lake Van Region. *Bulletin of the Mineral Research and Exploration*, 168, 141-156.
- Bayrak, Y., Yadav, R.B.S., Kalafat, D., Tsapanos, T.M., Çınar, H., Singh, A.P., Bayrak, E., Yılmaz, Ş., Öcal, F., Koravos, G., 2013. Seismogenesis and earthquake triggering during the Van (Turkey) 2011 seismic sequence. *Tectonophysics*, 601, 163-176.
- Bozkurt, E., 2001. Neotectonics of Turkey - a synthesis. *Geodin. Acta.*, 14, 3-30.
- Copley, A., Jackson, J., 2006. Active tectonics of the Turkish-Iranian Plateau. *Tectonics*, 25, TC6006.
- Delph, J., Biryol, C.B., Beck, S.L., Zandt, G., Ward, K.M., 2015. Shear wave velocity structure of the Anatolian Plate: anomalously slow crust in southwestern Turkey. *Geophys. J. Int.*, 202, 261-276.
- Djamour, Y., Vernant, P., Nankali, H.R., Tavakoli, F., 2011. NW Iran-eastern Turkey present-day kinematics: Results from the Iranian permanent GPS network. *Earth and Planetary Science Letters*, 307, 27-34.
- Elliott, J.R., Copley, A.C., Holley, R., Scharer, K., Parsons, B., 2013. The 2011 Mw 7.1 Van (Eastern Turkey) earthquake. *J. Geophys. Res. Solid Earth*, 118, 1619-1637.
- Emre, O., Duman, T.Y., Ozalp, S., Saroglu, F., Olgun, S., Elmaci, H., Can, T., 2018. Active fault database of Turkey. *Bulletin of Earthquake Engineering*, 16, 3229-3275.
- Frohlich, C., Davis, S., 1993. Teleseismic  $b$ -values: Or, much ado about 1.0. *J. Geophys. Res.*, 98(B1), 631-644.
- Gutenberg, B., Richter, F., 1944. Frequency of earthquakes in California. *B. Seismol. Soc. Am.*, 34, 185-188.
- Irmak, T.S., Doğan, B., Karakaş, A., 2012. Source mechanism of the 23 October, 2011, Van (Turkey) earthquake (Mw= 7.1) and aftershocks with its tectonic implications. *Earth Planets Space*, 64, 991-1003.
- King, G.C., Stein, R.S., Lin, J., 1994. Static stress changes and the triggering of earthquakes. *Bull. Seismol. Soc. Am.*, 84(3), 935-953.
- Koçyiğit, A., Yılmaz, A., Adamia, S., Kuloshvili, S., 2001. Neotectonics of East Anatolian Plateau (Turkey) and Lesser Caucasus: implication for transition from thrusting to strike-slip faulting. *Geodinamica Acta*, 14, 177-195.

- Mackenzie, D., Elliott, J.R., Altunel, E., Walker, R.T., Kurban, Y.C., Schwenninger, J.L., Parsons, B., 2016. Seismotectonics and rupture process of the M 7.1 2011 Van reverse-faulting earthquake, eastern Turkey, and implications for hazard in regions of distributed shortening. *Geophysical Journal International*, 206, 501-524.
- McClusky, S., Balassanian, S., Barka, A., Demir, C., Ergintav, S., Georgiev, I., Gurkan, O., Hamburger, M., Hurst, K., Kahle, H., Kastens, K., Kekelidze, G., King, R., Kotzev, V., Lenk, O., Mahmoud, S., Mishin, A., Nadariya, M., Ouzounis, A., Paradissis, D., Peter, Y., Prilepin, M., Reilinger, R., Sanli, I., Seeger, H., Tealeb, A., Toksöz, M.N., Veis, G., 2000. GPS constraints on plate motions and deformation in the Eastern Mediterranean: implications for plate dynamics. *J. Geophys. Res.*, 105, 5695-5719.
- Ottmøller, L., Voss, P.H., Havskov, J., 2021. SEISAN Earthquake Analysis Software for Windows, Solaris, Linux and MacOSx, Version 12.0. 607 pp. University of Bergen, ISBN 978-82-8088-501-2.
- Mogi, K., 1962. Magnitude-frequency relation for elastic shocks accompanying fractures of various materials and some related problems in earthquakes. *Bulletin of the Earthquake Research Institute, Tokyo University*, 40, 831-853.
- Ozer, C., Ozyaziciglu, M., Gök, E., Polat, O., 2019. Imaging the Crustal Structure Throughout the East Anatolian Fault Zone, Turkey, by Local Earthquake Tomography. *Pure Appl. Geophys.*, 176, 2235-2261.
- Öztürk, S., 2009. An application of the earthquake hazard and aftershock probability evaluation methods to Turkey earthquakes. PhD Thesis, Karadeniz Technical University, Trabzon, Turkey (in Turkish with English abstract).
- Öztürk, S., 2015. Fractal Dimension of Seismicity and a Modeling on the Intermediate-Term Forecasting for the Locations of Expected Strong Earthquakes: Eastern Anatolian Region, Turkey. *Gümüşhane University Journal of Science and Technology Institute*, 5(1), 1-23 (in Turkish with English abstract).
- Öztürk, S., 2017. Space-time assessing of the earthquake potential in recent years in the Eastern Anatolia region of Turkey. *Earth Sci. Res. J.*, 21, 2, 67-75.
- Öztürk, S., 2018. Earthquake hazard potential in the Eastern Anatolian Region of Turkey: seismotectonic b and Dc-values and precursory quiescence Z-value. *Front Earth Sci.*, 12(1), 215-236.
- Reasenber, P., Oppenheimer, D., 1985. Fpfit, Fpplot, and Fppage: Fortran computer programs for calculating and displaying earthquake fault plane solutions. Technical report, U.S. Geol. Survey.
- Reilinger, R., McClusky, S., Vernant, P., Lawrence, S., Ergintav, S., Cakmak, R., Ozener, H., Kadirov, F., Guliev, I., Stepanyan, R., Nadariya, M., Hahubia, G., Mahmoud, S., Sakr, K., ArRajehi, A., Paradissis, D., Al-Aydurs, A., Prilepin, M., Guseva, T., Evren, E., Dmitrova, A., Filikov, S.V., Gomez, F., Al-Ghazzi, R., Karam, G., 2006. GPS constraints on continental deformation in the Africa-Arabia-Eurasia continental collision zone and implications for the dynamics of plate interactions. *Journal of Geophysical Research Solid Earth*, 111(B5), B05411.
- Scholz, C.H., 2015. On the stress dependence of the earthquake b value. *Geophys. Res. Lett.*, 42, 1399-1402.
- Selçuk, A.S., Erturaç, M.K., Nomade, S., 2016. Geology of the Çaldıran Fault, Eastern Turkey: Age, slip rate and implications on the characteristic slip behaviour. *Tectonophysics*, 680, 155-173.
- Suetsugu, D., 1998. Practice on source mechanism, iisee lecture note. Technical report Tsukuba, Japan.
- Stein, R.S., King, G.C.P., Lin, J., 1994. Stress Triggering of the 1994 M = 6.7 Northridge, California, earthquake by its predecessors. *Science*, 265(5177), 1432-1435.
- Şaroğlu, F., 1986. Geological and structural evolution of East Anatolia during the Neotectonic period, Unpublished PhD Thesis, İstanbul University, Department of Geological Engineering, 240 page.
- Şaroğlu, F., Yılmaz, Y., 1986. Doğu Anadolu'da Neotektonik Dönemdeki Jeolojik Evrim ve Havza Modelleri, MTA Genel Müdürlüğü, Jeoloji Etütleri Dairesi, Ankara (in Turkish).
- Şengör, A.M.C., Ozeren, S., Genç, T., Zor, E., 2003. East Anatolian high plateau as a mantle-supported, north-south shortened domal structure. *Geophys. Res. Lett.*, 30, 24:8045.
- Reilinger, R., McClusky, S., Vernant, P., Lawrence, S., Ergintav, S., Cakmak, R., et al., 2006. GPS constraints on continental deformation in the Africa-Arabia-Eurasia continental collision zone and implications for the dynamics of plate interactions. *Journal of Geophysical Research: Solid Earth*, 111(B5).
- Toda, S., Stein, R.S., Sevilgen, V., Lin, J., 2011. Coulomb 3.3 Graphic-rich deformation and stress-change software for earthquake, tectonic, and volcano research and teaching-user guide. U.S. Geological Survey Open-File Report, 2011-1060, 63.
- Toker, M., Pınar, A., Hoşkan, N., 2021. An integrated critical approach to off-fault strike-slip motion triggered by the 2011 Van mainshock (Mw 7.1), Eastern Anatolia (Turkey): New stress field constraints on subcrustal deformation. *Journal of Geodynamics*, 147, 101861.
- Tsapanos, T.M., Bayrak, Y., Çınar, H., Koravos, G.C., Bayrak, E., Kalogirou, E.E., Tsapanou, V., Vougiouka, E., 2014. Analysis of Largest Earthquakes in Turkey and its Vicinity by Application of the Gumbel III Distribution. *Acta Geophysica*, 62, 1, 59-82.
- Utkucu, M., Durmuş, H., Yalçın, H., Budakoğlu, E., Işık, E., 2013. Coulomb static stress changes before and after the 23 October 2011 Van, eastern Turkey, earthquake (M = 7.1): implications for the earthquake hazard mitigation. *Nat. Hazards. Earth Syst. Sci.*, 13, 1889-1902.
- Wang, C., Ding, X., Li, Q., Shan, X., Zhu, W., Guo, B., Liu, P., 2015. Coseismic and postseismic slip models of the 2011 Van earthquake, Turkey, from InSAR, offset-tracking, MAI, and GPS observations. *Journal of Geodynamics*, 91, 39-50.
- Utsu, T., 1971. Aftershock and earthquake statistic (III): Analyses of the distribution of earthquakes in magnitude, time and space with special consideration to clustering characteristics of earthquake occurrence (1). *Journal of Faculty of Science Hokkaido University Series VII (Geophysics)* 3, 379-441.
- Wessel, P., Smith, W.H.F., Scharroo, R., Luis, J.F., Wobbe, F., 2013. Generic mapping tools: improved version released. *EOS Transaction AGU*, 94, 409-410.
- Wiemer, S., Wyss, M., 2000. Minimum magnitude of completeness in earthquake catalogs: Examples from Alaska, the Western United States, and Japan. *B. Seismol. Soc. Am.*, 90(3), 859-869.
- Wiemer, S., 2001. A software package to analyze seismicity: ZMAP. *Seismological Research Letters*, 72(3), 373-382.
- Yadav, R.B.S., Gahalaut, V.K., Chopra, S.B., 2012. Tectonic implications and seismicity triggering during the 2008 Baluchistan, Pakistan earthquake sequence. *J. Asian Earth Sci.*, 45, 167-178.
- Yiğitbaş, E., Elmas, A., Sefunç, A., Özer, N., 2004. Major neotectonic features of eastern Marmara region, Turkey: development of the Adapazarı-Karasu corridor and its tectonic significance. *Geological Journal*, 39, 179-198.

URL-1 . <https://depem.afad.gov.tr/ddakatalogu>, Accessed 2022.

URL-2 <https://earthquake.usgs.gov/earthquakes/map>, Accessed 2022.

URL-3 <http://www.koeri.boun.edu.tr/sismo/2/earthquake-catalog>, Accessed 2022.